Search for WIMP annual modulation signature: results from DAMA/NaI-3 and DAMA/NaI-4 and the global combined analysis

R. Bernabei [a], P. Belli [a], R. Cerulli [a], F. Montecchia [a], M. Amato [b], G. Ignesti [b], A. Incicchitti [b], D. Prosperi [b], C.J. Dai [c], H.L. He [c], H.H. Kuang [c], J.M. Ma [c]

[a] *Dip. di Fisica, Universita' di Roma ''Tor Vergata'' and INFN, sez. Roma2, I-00133 Rome, Italy*
[b] *Dip. di Fisica, Universita' di Roma ''La Sapienza'' and INFN, sez. Roma, I-00185 Rome, Italy*
[c] *IHEP, Chinese Academy, P.O. Box 918 / 3, Beijing 100039, China*

Abstract

Data, collected by the $\simeq 100$ kg NaI(Tl) DAMA set-up at the Gran Sasso National Laboratory of I.N.F.N. during two further yearly cycles (DAMA/NaI-3 and DAMA/NaI-4; statistics of 38475 kg · day), have been analysed in terms of WIMP annual modulation signature. The results agree with those previously achieved. The cumulative analysis of all the available data (DAMA/NaI-1 to 4; statistics of 57986 kg · day) favours the possible presence of a WIMP with $M_w = (52^{+10}_{-8})$ GeV and $\xi\sigma_p = (7.2^{+0.4}_{-0.9}) \cdot 10^{-6}$ pb at 4 σ C.L., when standard astrophysical assumptions are considered. The allowed mass extends up to 105 GeV (1 σ) when the uncertainty on the mean value of the local velocity v_0 is taken into account and up to 132 GeV (1 σ) in case a possible bulk halo rotation is taken into account. Moreover, the allowed regions extend to lower $\xi\sigma_p$ values when the upper limits on the recoil differential counting rate obtained from DAMA/NaI-0 is included in the cumulative analysis (favouring, in case of standard assumptions, $M_w = (44^{+12}_{-9})$ GeV and $\xi\sigma_p = (5.4 \pm 1.0) \cdot 10^{-6}$ pb at $\simeq 4$ σ C.L.). The 3 σ C.L. allowed regions in the $\xi\sigma_p$, M_w plane summarize the obtained main physical results. © 2000 Elsevier Science B.V. All rights reserved.

1. Introduction

The $\simeq 100$ kg NaI(Tl) DAMA set-up is running at the Gran Sasso National Laboratory of I.N.F.N. [1–11]; its main goal is to search for Weakly Interacting Massive Particles (WIMPs). According to standard models, these particles would have in the galactic halo a Maxwellian velocity distribution with a cut-off at the galactic escape velocity; therefore, a WIMP ''wind'' would continuously hit the Earth.

WIMPs can be detected by investigating their elastic scattering on the target nuclei of a detector. The nuclear recoil energy in the keV range is the measured quantity. The best way to single out the possible presence of a WIMP signal from the background is to look for the so-called *annual modulation signature* [4–6,12,13]. In fact, since the Earth rotates around the Sun, it would be invested by a larger WIMP flux in June (when its rotational velocity adds up to the velocity of the whole solar system in the

Galaxy) and by a smaller flux in December (when the two velocities are in opposite directions), inducing a peculiar modulation of the low energy counting rate [4–6,12,13]. A WIMP induced effect should fulfill all the following requirements: i) modulation of the "single hit" rate [1]; ii) for events only in a well defined low energy region; iii) according to a cosine-like behaviour; iv) with a one year period (T); v) with a phase $t_0 \simeq 2$ June (corresponding to the $\simeq 152.5$th day of the year); vi) and limited modulated amplitude ($\lesssim 7\%$ in the region of maximal sensitivity).

At present the lightest supersymmetric particle named neutralino, whose interaction with ordinary matter is mainly spin-independent (SI), is considered the best candidate for WIMP; in the following we will devote particular attention to this case (see Sections 4 and 5).

Investigations exploiting statistics of 4549 kg · day (DAMA/NaI-1) and of 14962 kg · day (DAMA/NaI-2) have been already presented in Refs. [4–6], while the possible implications have been discussed in Refs. [14–16].

The detailed description of the DAMA set up and its performances have been presented in Ref. [1], where the radiopurity of all its components has also been discussed. Moreover, in Refs. [6,17,18] some specific considerations on the realization of radiopure NaI(Tl) detectors have been addressed. The data were collected by means of nine 9.70 kg NaI(Tl) crystal scintillators in suitably radiopure Cu housings. Each detector has two 10 cm long tetrasil-B light guides directly coupled to the opposite sides of the bare crystal. Two low background photomultipliers work in coincidence and collect light at single photoelectron threshold; 2 keV is the used software energy threshold [1,2,4–6,11]. The detectors are housed in a low radioactive sealed copper box inside a low radioactive multicomponent shield (paraffin/polyethylene/Cd foils/Pb/Cu) from environmental background. A high purity (HP) Nitrogen atmo-

sphere – at slight overpressure with respect to the external environment – is maintained inside the copper box by a continuous flux of HP Nitrogen gas from bottles stored underground since time. The whole shield is also sealed and maintained in HP Nitrogen atmosphere; particular care was also devoted to obtain an experimental site as much air-tight as possible. The installation is subjected to air conditioning to avoid any significative influence of the temperature (see Refs. [1,4–6] and later).

2. DAMA/NaI-3 AND DAMA/NaI-4 data and stability controls

The DAMA/NaI-3 data were collected roughly from middle August 1997 to the end of September 1998 (22455 kg · day statistics), while DAMA/NaI-4 refers to data collected roughly from middle October 1998 until the second half of August 1999 (16020 kg · day statistics) [2].

The typical differential counting rate in the region between 2 and 20 keV has been previously reported in Refs. [4,5,8]; the cumulative data referring to the energy interval between $\simeq 1$ and 10 keV have been reported [3] in Ref. [11]; the shapes of the energy distribution of each detector are quite similar. Moreover, parts of the cumulative energy spectrum for larger energies have also been presented in Ref. [9]. For completeness, Fig. 1 shows the cumulative energy spectrum near the used 2 keV software energy threshold for the data of the two yearly cycles considered here.

We recall that the rejection of residual noise near energy threshold is performed exploiting the distributions – different for scintillation pulses (signals with decay times of order of hundreds ns) and noise

---

[1] When searching for WIMPs with a multi-detector set-up (as DAMA/NaI), the low energy rates are always referred to events where only one detector is firing ("single hit" events), being negligible the probability that a WIMP will interact in more than one.

[2] Some upgradings have been performed before the DAMA/NaI-4 running period.

[3] This is the region of maximal interest to search for SI coupled WIMPs because of: i) the quasi-exponential energy distribution of the induced nuclear recoils; ii) the possible annual modulation effect singled out in the lowest energy bins in Refs. [4–6]; iii) the location of the first pole of the Iodine form factor [19]. Note that the software energy threshold has been so far cautiously taken at 2 keV to assure a full noise rejection near it with the used strategy [1].
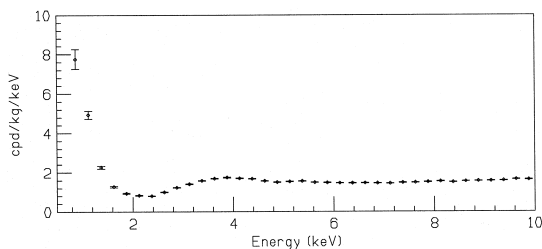
Fig. 1. Cumulative energy spectrum near the used 2 keV software energy threshold (DAMA/NaI-3 and DAMA/NaI-4 data). This distribution refers – as usual in our experiment – to ''single hit'' events (that is each detector has all the others as veto).

pulses (PMT fast signals with decay times of order of tens ns) – of several variables built by using the information recorded over 3250 ns by a Lecroy Transient Digitizer [1,2,4,5]; examples of these distributions as well as the evaluation of the corresponding software cut efficiencies can be found in Ref. [1]. In particular, as mentioned there, very stringent cuts are applied near energy threshold to exclude the presence of any significant tail of residual noise after rejection.

The stability of the efficiencies over the whole data taking periods has been investigated. Their possible time variation depends essentially on the stability of the so-called cut efficiencies (see Ref. [1]). The latters are regularly measured by ^{241}Am source and ^{137}Cs Compton electron calibrations (as mentioned in Ref. [1] the obtained values resulted practically the same). These routine efficiency measurements are performed roughly each 10 days, collecting each time typically 10^4–10^5 events each keV. In particular, we have investigated the percentage variations of the efficiency values, e.g. in the (2–8) keV energy interval; they show a gaussian distribution with $\sigma =$ 0.6% and 0.5% for DAMA/NaI-3 and DAMA/NaI-4, respectively. Moreover, we have verified that the time behaviour of these percentage variations does not show any modulation with period and phase expected for a possible WIMP signal. In particular, in the (2–4) keV energy interval a modulated amplitude (taking the two periods all together) equal to $(1.0 \pm 1.0) \cdot 10^{-3}$ is found, while in the (4-6) keV the result is $(0.1 \pm 0.7) \cdot 10^{-3}$, they are both consistent with zero. Similar results are obtained in other energy bins.

In long term running conditions, the knowledge of the energy scale is assured by periodical calibration with ^{241}Am source and by continuously monitoring within the same production data (grouping them each $\simeq 7$ days) the position and resolution of the ^{210}Pb peak [4] (46.5 keV) [1,4,5]. As in Refs. [5,6], the distribution of the relative variations of the energy calibration factors, estimated from the position of the $_{210}$Pb peak for all the 9 detectors during both DAMA/NaI-3 and DAMA/NaI-4 taken without any correction, has been investigated; it shows a gaussian behaviour with $\sigma = (0.95 \pm 0.04)$%. Since the results of the routine calibrations are obviously properly taken into account in the data analysis, such a result allows to conclude that the energy calibration factors for each detector are known with an uncertainty < 1%. Due to the relatively poor energy resolution of the detectors at low energy, this could give rise only to an additional relative energy spread $\lesssim 10^{-4}$ in the lowest energy region and $\lesssim 10^{-3}$ at 20 keV, totally negligible.

All the relevant stability parameters have been quantitatively investigated for each data set, obtaining time behaviours like the ones shown in Refs. [4–6]. In particular, as already discussed in Refs. [1,5,6], the observed variations of the temperature can only induce a practically negligible variation of the light output, in agreement with the results obtained by the long term routine and intrinsic calibrations [1,4,5]. Furthermore, as already discussed in Refs. [1,4–6], the detectors are *excluded* from the environmental Radon being housed in a sealed Cu box which is continuously flushed with a large flux of high purity (HP) N_2 and maintained at a slight overpressure with respect to the environment [1,4,5] (see also Section 1). In addition, the observed time behaviour of the external Radon level allows to exclude the presence in it of a cosine-like modulated component with period and phase expected for a WIMP signal; in fact, a fit gives for its amplitude the values (0.14 ± 0.25) Bq/m^3 during DAMA/NaI-3

---

[4] It is present at level of few cpd/kg in the measured energy distributions, mainly because of a surface contamination by environmental Radon occurred during the first period of the detectors storage underground.

and (0.12 ± 0.20) Bq/m^3 during DAMA/NaI-4, both evidently consistent with zero.

The distribution of the total hardware rate of the nine detectors (R_H) above the single photoelectron threshold (i.e. from noise to ''infinity'') has also been investigated; it shows a gaussian behaviour with $\sigma = 0.6\%$ for DAMA/NaI-3 and $\sigma = 0.4\%$ for DAMA/NaI-4, values which are in agreement with those expected on the basis of simple statistical arguments. Furthermore, no evidence for time modulation of R_H has been found.

The measured energy distributions in energy regions not involved in the Dark Matter direct detection for DAMA/NaI-3 and DAMA/NaI-4 have been investigated as a function of the time in order to exclude that a modulation detected in the lowest energy region could be due to a background modulation [5]. For this purpose, according to Refs. [5,6], we have investigated the rate integrated from 90 keV to ''infinity'', R_{90}, as a function of time. The distributions of the percentage variations of R_{90} with respect to their mean values for all the crystals during both DAMA/NaI-3 and DAMA/NaI-4 show a gaussian behaviour with $\sigma \simeq 1.3\%$ and $\sigma \simeq 1.0\%$, respectively, values well accounted for the expected statistical spread. Moreover, fitting the time behaviour of R_{90} by also adding a term modulated according to a cosine function with 1 year period and 152.5 day phase (as expected for a WIMP signal), the value (-0.11 ± 0.33) cpd/kg is found for the modulated amplitude in the DAMA/NaI-3 data and (-0.35 ± 0.32) cpd/kg in the DAMA/NaI-4 ones, both consistent with zero. These results allow to exclude the presence of a background modulation in the whole energy spectrum at a much lower level than the possible signal modulation found in the lowest energy region (see Refs. [4,5] and later); in fact, otherwise, the modulated amplitude for R_{90} would be of

order of tens cpd/kg, that is $\simeq 100$ standard deviations away from the measured value. Finally, focusing the attention on the energy region nearer to the one where the possible signal has been detected [4,5], e.g. 10–20 keV, the values (-0.0044 ± 0.0044) cpd/kg/keV and (-0.0071 ± 0.0044) cpd/kg/keV have been found for the modulated amplitude in DAMA/NaI-3 and in DAMA/NaI-4, respectively; again they can be considered statistically consistent with zero.

The quantitative investigations reported in this section offer a complete analysis of the possible sources of systematic effects, which could affect the energy spectrum. These investigations credit a percentage systematic error $\lesssim 10^{-3}$ on the basis of the measured variations of temperature, calibration uncertainties, etc. Moreover, the results on the analysis of R_{90} exclude at an even more stringent level the presence of a possible overall background modulation (excluding also significant contribution e.g. from possibly surviving neutrons from the environment). Finally, no contribution can arise from environmental Radon, as the detectors are excluded from it (in addition, a time correlation analysis offers, as mentioned, a Radon modulated contribution compatible with zero).

We want to point out here that really the only dangerous systematic effects are those that satisfy the same six requirements a WIMP induced effect is expected to fulfill (see Section 1); no systematic effect of this type has been found so far. The same should also be true for possible competing physical processes; the only one we found up to now: the muon modulation reported in Ref. [20], would fail on some of them, it would yield a modulation in R_{90} (which is not observed) and – in any case – it would give in our set-up modulated amplitudes $\ll 10^{-4}$ cpd/kg/keV, much lower than we observe. So it can be safely ignored.

In conclusion, the results presented in this section allow to perform a statistical analysis of the data.

---

[5] In fact, the background in the lowest energy region is expected to be essentially due to Compton electrons, X-rays and/or Auger electrons, muon induced events, etc., which are strictly correlated with the events in the higher energy part of the spectrum; therefore, if a detected modulation with time in the lowest energy region would be due to a background modulation (and not to a possible real signal), an equal or higher (sometimes much higher) modulation in the highest energy region should also be present.

3. Model independent approach: a visual aid

As mentioned, the results discussed in the previous section allow to investigate the events in the lowest energy part of the energy spectrum in terms

of WIMP annual modulation signature. A complete analysis [4,5] will be carried out in the following sections, properly taking into account the energy and time differential distribution of the events. Here, in order to offer an immediate evidence of the presence of modulation in the lowest energy region of the experimental data, we show as an example in Fig. 2 the model independent residual rate for the cumulative 2–6 keV energy interval as a function of the time over the present full data taking period of our experiment (DAMA/NaI-1 to DAMA/NaI-4) [6]. Each data point has been obtained from the raw rate after subtracting the constant part (the weighted mean of the residuals must obviously be zero over one period), so we plot $< r_{ijk} - \text{flat}_{jk} >_{jk}$. Moreover, r_{ijk} is the rate in the considered i-th time interval for the j-th detector in the k-th energy bin, while flat$_{jk}$ is the rate of the j-th detector in the k-th energy bin averaged over the cycles. The average is made on all the detectors (j index) and on all the 1 keV bins (k index) which constitute the considered energy interval.

The χ^2 test on the data of Fig. 2 disfavours the hypothesis of unmodulated behaviour giving a probability of $4 \cdot 10^{-4}$ ($\chi^2/\text{d.o.f.} = 48/20$). On the other hand, fitting these residuals with the function $A \cdot \cos \omega(t - t_0)$ (obviously integrated in each of the considered time bin), one gets $A = (0.022 \pm 0.005)$ cpd/kg/keV, $T = 2\pi/\omega = (1.00 \pm 0.01)$ year, when fixing t_0 at 152.5 days and $A = (0.023 \pm 0.005)$ cpd/kg/keV, $t_0 = (144 \pm 13)$ days, when fixing T at 1 year. In both cases $\chi^2/\text{d.o.f.} \simeq 23/18$. Similar results, but with larger errors, are found in case all the three parameters are kept free. As it is evident the period and the phase fully agree with the ones expected for a WIMP induced effect.

Let us now investigate the data with the complete needed sensitivity for WIMP mass and cross-section determination. At the end of Section 5 we will

---

[6] The bins considered in this figure for DAMA/NaI-3 and DAMA/NaI-4 are similar to those previously used for DAMA/NaI-1 and DAMA/NaI-2. We have verified that the results of this approach are substantially unchanged by choosing other bins for the presentation. Moreover, we further stress that this presentation is only a visual aid, as the final results obtained through the full correlation analysis in time (1 day bin) and energy (1 keV bin) is carried out in the following sections.
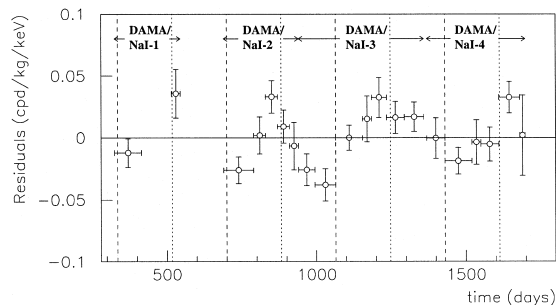

Fig. 2. Model independent residual rate in the particular 2-6 keV cumulative energy interval as a function of the time elapsed since January 1-st of the first year of data taking. The expected behaviour of a WIMP signal is a cosine function with minimum roughly at the dashed vertical lines and with maximum roughly at the dotted ones.

further comment on this approach, still using this particular 2–6 keV cumulative interval as an example.

4. Full correlation analysis of the DAMA/NaI-3 and DAMA/NaI-4 data sets

According to Refs. [4,5], a complete time and energy correlation analysis of the data collected between 2 and 20 keV has been performed by using the standard maximum likelihood method. For this purpose the data have been grouped in cells identified by three indices: i for the time interval (1 day), k for the energy bin ($\Delta E = 1$ keV) and j to specify the detector. The maximum likelihood function can be written as a product of Poissonians $\mathbf{L} = \mathbf{\Pi}_{ijk} e^{-\mu_{ijk}} \frac{\mu_{ijk}^{N_{ijk}}}{N_{ijk}!}$. Here N_{ijk} is the number of events in each ijk cell which follows a Poissonian distribution with expectation value $\mu_{ijk} = [b_{jk} + S_{0,k} + S_{m,k} \cdot \cos \omega(t_i - t_0)]M_j \Delta t_i \Delta E \epsilon_{jk}$. The unmodulated and modulated parts of the signal are $S_{0,k}$ and $S_{m,k} \cos \omega(t_i - t_0)$, respectively; b_{jk} is the background contribution; Δt_i is the detector running time during the i-th day ($\Delta t \leq 1$ day); ϵ_{jk} are the overall efficiencies discussed in Ref. [1] and M_j is the detector mass.

Furthermore, according to: i) the formulae for the calculation of the recoil energy spectrum; ii) the measured quenching factors; iii) the form factors; iv) the folding of the detector response, given in Refs.

[2,4,5], we can make explicit the $S_{0,k}$ and $S_{m,k}$ dependence on M_w (the WIMP mass) and $\xi\sigma_p$ ($\xi = \frac{\rho_{\text{WIMP}}}{0.3\,\text{GeV cm}^{-3}}$; σ_p = WIMP scalar cross section on proton) by writing $S_{0,k} = \xi\sigma_p S'_{0,k}(M_w)$ and $S_{m,k} = \xi\sigma_p S'_{m,k}(M_w)$. Therefore, $\mathbf{L}$ will be a function of b, M_w and $\xi\sigma_p$ for a given N: $\mathbf{L} = \mathbf{L}(N; b, M_w, \xi\sigma_p)$, where by N we have for short indicated the whole set of N_{ijk} and, similarly, by b the set of all the b_{jk}. The maximum likelihood estimates of the parameters b, M_w and $\xi\sigma_p$ are obtained by maximizing $\mathbf{L}$ for a given set of observations, N, or by minimizing the function: $y = -2\ln(\mathbf{L}) - \text{const}$, with const chosen so as to have $y(\sigma_p = 0) = 0$ [4,5]. The constraints imposed on the minimization procedure [4,5] are: $b_{jk} \geq 0$ and $M_w \geq 30$ GeV; the latter condition accounts for the more recent results achieved in accelerator experiments for the neutralino mass. In the minimization procedure the WIMP mass has been varied up to 10 TeV.

As usual in particle Dark Matter direct searches [21], standard hypotheses have been used in the calculations of the distribution of astrophysical velocities [4,5], while a detailed investigation of the effects induced by their uncertainties [22] has been performed in Ref. [7]. In this last reference it was shown that the uncertainties on the expected local velocity v_0, as well as a possible bulk halo rotation, can play a significant role. In the following, for simplicity, the analysis of a single set (DAMA/NaI-3 or DAMA/NaI-4) will be performed by considering the standard value $v_0 = 220$ km/s, while the uncertainty on v_0 will be considered in the global analysis of all the available data (DAMA/NaI-1 to 4).

By assuming the same standard astrophysical, nuclear and particle physics hypotheses employed in Refs. [2,4,5], the minimum value of the y function is obtained for the DAMA/NaI-3 data when $M_w = (56^{+18}_{-26})$ GeV, $\xi\sigma_p = (9.7^{+0.3}_{-3.5})10^{-6}$ pb and, for the DAMA/NaI-4 data, when $M_w = (44^{+32}_{-14})$ GeV, $\xi\sigma_p = (6.9^{+3.9}_{-3.8})10^{-6}$ pb.

The likelihood of the null hypothesis (absence of modulation) with respect to the hypothesis of presence of modulation with the fitted M_w and $\xi\sigma_p$ values has been tested for both periods by the maximum likelihood ratio [4,5], obtaining that the hypothesis of presence of modulation with such M_w and $\xi\sigma_p$ values is favoured at 98.3% C.L. for the DAMA/NaI-3 data and at 92.8% C.L. for the

DAMA/NaI-4 data. Moreover, the likelihood of the hypothesis of presence of modulation with the values of M_w and $\xi\sigma_p$ obtained from the fit has been studied, according to the approach of Ref. [23], by constructing the variable $z = \frac{1}{N} \cdot \Sigma_{ijk}[2(\mu_{ijk} - N_{ijk}) + 2N_{ijk}\ln\left(\frac{N_{ijk}}{\mu_{ijk}}\right)]$ where N is the total number of ijk cells. From experimental data z comes out to be respectively 1.036 for DAMA/NaI-3 and 1.009 for the DAMA/NaI-4. The MonteCarlo distribution of z, evaluated as in Ref. [5], gives a 19% probability to get a z value larger than 1.036 for DAMA/NaI-3 and 99.8% probability to get a z value larger than 1.009 for DAMA/NaI-4. Moreover, the z-test separately applied to the data of each detector shows that the modulation is confirmed at 95% C.L. in both data sets. Alternative analyses such as the one based on the χ_{test} variable described in Ref. [5] offer substantially the same results.

In Fig. 3 the regions allowed at 90% C.L. – for a SI coupled candidate – for the $\xi\sigma_p$ and M_w values obtained under standard assumptions by analysing the DAMA/NaI-3 (c) and DAMA/NaI-4 (d) data are shown superimposed to the ones credited by DAMA/NaI-1 (a) and DAMA/NaI-2 (b) [4,5]. The 90% C.L. contour curve obtained in Ref. [2] (DAMA/NaI-0) is also reported. We take this occasion to recall that the DAMA/NaI-0 data are par-
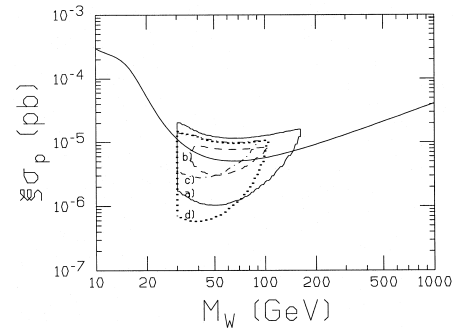

Fig. 3. Regions allowed at 90% C.L. – for a SI coupled candidate – by the $\xi\sigma_p$ and M_w values obtained for DAMA/NaI-3 (c) and for DAMA/NaI-4 (d) data superimposed to the ones credited by DAMA/NaI-1 (a) and DAMA/NaI-2 (b) [4,5]. The calculations have been performed according to the same astrophysical, nuclear and particle physics considerations as in Refs. [4,5]; in particular – as usual in particle Dark matter direct searches [21] – here the standard value $v_0 = 220$ km/s has been used. The limit curve at 90% C.L. achieved in Ref. [2] (DAMA/NaI-0) is also shown.

tially overlapped to the DAMA/NaI-1 data and have been analysed in Ref. [2] in terms of pulse shape discrimination.

5. Full correlation analysis of all the available data sets

In this section we report the analysis performed with the standard maximum likelihood method of all the available data. They refer to four different yearly cycles (DAMA/NaI-1 to DAMA/NaI-4) and the total statistics is 57986 kg · day.

Using the same strategy as in the previous section and in Refs. [4,5] (in particular, $v_0 = 220$ km/s), the minimum value of the y function is found for $M_w = (52^{+10}_{-8})$ GeV and $\xi\sigma_p = (7.2^{+0.4}_{-0.9})10^{-6}$ pb. The maximum likelihood ratio favours the hypothesis of presence of modulation with these values of M_w and $\xi\sigma_p$ at $4\ \sigma$ C.L. The $S_{0,k}$ and $S_{m,k}$, obtained using the results of the maximum likelihood method, are shown up to 6 keV in Table 1 (above this energy S_m values are negligible).

As in Refs. [7,18], the minimization procedure has been repeated by varying v_0 from 170 km/s to 270 km/s [22] to account for its present uncertainty and, also, to include possible bulk halo rotation.

We show in Fig. 4a) the regions allowed at 3σ C.L. when: i) $v_0 = 220$ km/s (dotted contour); ii) the uncertainty on v_0 is taken into account (continuous contour); iii) possible bulk halo rotation is considered (dashed contour). They are well inside the Minimal Supersymmetric Standard Model (MSSM) estimates for the neutralino [14].
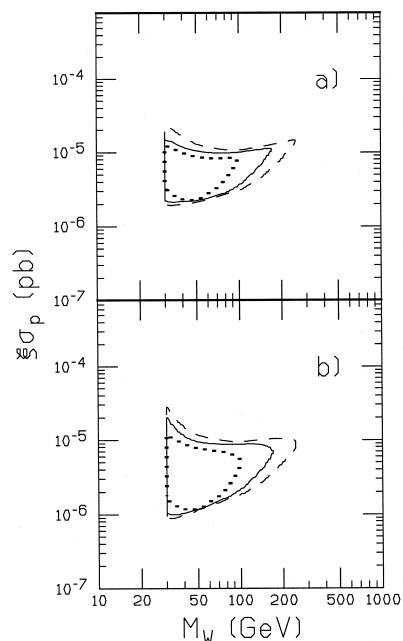

Fig. 4. a) Regions allowed at 3σ C.L.: i) for $v_0 = 220$ km/s (dotted contour); ii) when accounting for v_0 uncertainty (170 km/s $\leq v_0 \leq$ 270 km/s; continuous contour); iii) when considering also a possible bulk halo rotation as in Ref. [7] (dashed contour); b) Regions allowed at 3σ C.L. – for the same conditions as previously reported – when including the constraint arising from the upper limits on the recoil differential counting rate obtained in Ref. [2] (DAMA/NaI-0).

At this point we have repeated the minimization procedure taking into account the constraint which arises from the upper limits on the recoil differential counting rate obtained in Ref. [2] (DAMA/NaI-0).

Table 1
$S_{0,k}$ and $S_{m,k}$ values in the region of maximum interest for the possible signal as obtained by using the results of the global analysis for DAMA/NaI-1 to DAMA/NaI-4 with $v_0 = 220$ km/s and including or not the constraint arising from the results of DAMA/NaI-0 [2] (see text)

Energy (keV)	Without constraint from DAMA/NaI-0		With constraint from DAMA/NaI-0	
	$S_{0,k}$ (cpd/kg/keV)	$S_{m,k}$ (cpd/kg/keV)	$S_{0,k}$ (cpd/kg/keV)	$S_{m,k}$ (cpd/kg/keV)
2–3	0.54 ± 0.09	0.023 ± 0.006	0.36 ± 0.10	0.021 ± 0.005
3–4	0.21 ± 0.05	0.013 ± 0.002	0.12 ± 0.05	0.010 ± 0.002
4–5	0.08 ± 0.02	0.007 ± 0.001	0.04 ± 0.02	0.004 ± 0.001
5–6	0.03 ± 0.01	0.003 ± 0.001	0.02 ± 0.01	0.002 ± 0.001

In this case, the maximum likelihood function is given by the unconstrained one (defined above) times

$$\mathbf{L}_0 = \frac{1}{\sqrt{2\pi} \cdot \sigma_k} \cdot \exp\left(- \frac{\left(r_k - b_k^0 - S_{0,k}\right)^2}{2\sigma_k^2} \right),$$

where r_k and σ_k are the lowest counting rate and the associated error in the most selective energy bin of the data in Ref. [2] [7]. Moreover, for each M_w and $\xi\sigma_p$ the fitted value of b_k^0, which maximizes $\mathbf{L}_0$, is: $b_k^0 = (r_k - S_{0,k}) \cdot \theta(r_k - S_{0,k})$, considering the condition that it cannot be negative. Therefore, the term added to the function y can be re-written as: $\frac{(S_{0,k} - r_k)^2}{\sigma_k^2} \cdot \theta(S_{0,k} - r_k)$. The Heaviside θ function ensures that the term added to the function y contributes only when the expected value for $S_{0,k}$ is larger than r_k. In this way the minimum value of the y function – when $v_0 = 220$ km/s – is found for $M_w = (44^{+12}_{-9})$ GeV and $\xi\sigma_p = (5.4 \pm 1.0) \cdot 10^{-6}$ pb. The maximum likelihood ratio favours the hypothesis of presence of modulation with these values of M_w and $\xi\sigma_p$ at $\simeq 4\sigma$ C.L.; the corresponding $S_{0,k}$ and $S_{m,k}$ values can be found in Table 1.

In Fig. 4b) we show the regions allowed in this case at 3σ C.L. when: i) $v_0 = 220$ km/s (dotted contour); ii) the uncertainty on v_0 is taken into account (continuous contour); iii) possible bulk halo rotation is considered (dashed contour).

The confidence levels quoted above have been also verified by suitable MonteCarlo calculations; in particular, we note that the Feldman and Cousins analysis [24] of the data gives quite similar results.

Finally, to clearly show the relevance of performing a full correlation analysis (as the standard maximum likelihood considered above) able to properly account for all the features of the time and energy differential distribution of the measured events, we come back to the simple approach of Section 3, where the particular cumulative 2–6 keV energy

interval has been taken as an example. For this purpose, in Table 2 we report the χ^2/d.o.f. and the relative probabilities obtained by comparing the residuals of Fig. 2 with the values expected when considering the M_w and $\xi\sigma_p$ values relative to the minima obtained by the cumulative analysis under standard assumptions, either taking into account (b) or not taking into account (a) the constraint from DAMA/NaI-0 data. As one can see in both cases, a good agreement for DAMA/NaI-1, DAMA/NaI-2 and DAMA/NaI-4 is found, while the agreement is poorer for DAMA/NaI-3. This is due to the first two DAMA/NaI-3 points in Fig. 2, as shown by the substantial change of χ^2/d.o.f. (and probability value) one gets if they are left out of the analysis. Moreover, their fluctuation appears to be significant only in one of the involved energy bins (tails of distributions sometimes can play a role); in fact, if

Table 2

Comparison of the residuals in the cumulative 2–6 keV energy interval (given as an example in Fig. 2) with the values expected when considering the M_w and $\xi\sigma_p$ values of the minima obtained – under standard assumptions – by the cumulative analysis either considering (b) or not (a) the constraint from DAMA/NaI-0. As one can see in these cases, a good agreement is present for DAMA/NaI-1, DAMA/NaI-2 and DAMA/NaI-4, while it is poorer for DAMA/NaI-3 owing to its first two points. The fluctuation of these two residual points is present there in only one of the involved energy bins (obviously in statistics the tails can also play some role). In fact, if, e.g., the 2–5 keV (where most of the signal is expected) residuals would be indeed considered, the χ^2/d.o.f. values (when taking into account all the residuals over the four yearly cycles) would be 11.5/20 (93% probability) and 12.3/20 (91% probability), respectively. This clearly shows the relevance of performing a complete analysis approach able to properly take into account all the features of the time and energy differential distribution of the events, giving also a C.L. which accounts for the whole behaviour, as it is the standard maximum likelihood method we use

	χ^2/d.o.f. (probability)	
	case a)	case b)
DAMA/NaI-1	1.7/2 (43%)	2.1/2 (35%)
DAMA/NaI-2	6.8/5 (23%)	7.7/5 (17%)
DAMA/NaI-3	14.4/7 (4.5%)	15.4/7 (3.2%)
without first 2 points	4.9/5 (43%)	5.3/5 (38%)
DAMA/NaI-4	6.1/6 (42%)	6.5/6 (37%)
DAMA/NaI-1 to 4	29.0/20 (9%)	31.6/20 (4.7%)
without the first 2 points of DAMA/NaI-3	19.5/18 (36%)	21.6/18 (25%)

---

[7] In the formulation of $\mathbf{L}_0$ the term $S_{m,k} \cdot <\cos\omega(t - t_0)>$ has been neglected with respect to $S_{0,k}$ (which is the usual approach in the calculation of exclusion plots). Furthermore, we have verified that introducing the contributions of the other energy bins and of the other detectors the results are substantially unchanged as expected.

the residuals in the cumulative 2–5 keV energy interval (where most of the signal is expected) are indeed considered, the χ^2/d.o.f. values (when taking into account all the residuals over the four cycles) come out to be 11.5/20 (93% probability) and 12.3/20 (91% probability), respectively.

At this point, we wish to notice that, as for the case of v_0 and possible bulk rotation, uncertainties can also arise from standard nuclear and particle physics assumptions used in the evaluation of S_0 and S_m. As an example we mention the case of the form factor, which depends on the nuclear radius and on the thickness parameter of the nuclear surface [19]. For instance, we have verified that by varying their values with respect to the standard ones by 20%, the locations of the minima will move toward slightly larger M_w and toward lower $\xi\sigma_p$ values, while the calculated S_m, if integrated in the 2–6 keV energy interval, discussed above, will increase by about 15%.

6. Conclusions

The data collected over four yearly cycles (total statistics of 57986 kg · day) favour at 4 σ C.L. the presence of an annual modulation in the low energy experimental rate, measured deeply underground at the Gran Sasso National Laboratory by the $\simeq 100$ kg highly radiopure NaI(Tl) DAMA set-up. Here this effect has been further investigated in terms of possible relic neutralinos; the 3 σ C.L. allowed contours in the $\xi\sigma_p$, M_w plane have been given.

The experiment keeps on running and an upgrading of the electronics has been prepared to verify further peculiarities of the effect to deeply investigate its nature. In incoming years the exposed mass will be increased up to 250 kg.

References

[1] R. Bernabei et al., Il Nuovo Cim. A 112 (1999) 545.
[2] R. Bernabei et al., Phys. Lett. B 389 (1996) 757.
[3] R. Bernabei et al., Phys. Lett. B 408 (1997) 439.
[4] R. Bernabei et al., Phys. Lett. B 424 (1998) 195.
[5] R. Bernabei et al., Phys. Lett. B 450 (1999) 448.
[6] R. Bernabei et al., in the volume ''3K-Cosmology'', AIP pub., 1999, p. 65.
[7] P. Belli et al., hep-ph/9903501; Phys. Rev. D 61 (2000) 023512.
[8] P. Belli et al., Phys. Lett. B 460 (1999) 236.
[9] P. Belli et al., Phys. Rev. C 60 (1999) 065501.
[10] R. Bernabei et al., Phys. Rev. Lett. 83 (1999) 4918.
[11] R. Bernabei et al., Il Nuovo Cim. A 112 (1999) 1541.
[12] K.A. Drukier et al., Phys. Rev. D 33 (1986) 3495.
[13] K. Freese et al., Phys. Rev. D 37 (1988) 3388.
[14] A. Bottino et al., Phys. Lett. B 423 (1998) 109; Phys. Rev. D 59 (1999) 095004; Phys. Rev. D 59 (1999) 095003; Astrop. Phys. 10 (1999) 203; hep-ph/9909228 to appear in Astrop. Phys.
[15] R.W. Arnowitt, P. Nath, Phys. Rev. D 60 (1999) 044002.
[16] D. Fargion et al., Pis'ma Zh. Eksp. Teor. Fiz. 68 (JETP Lett. 68, 685) (1998); to appear on Astrop. Phys.
[17] I.R. Barabanov et al., Nucl. Phys. B 546 (1999) 19.
[18] R. Bernabei, in: M. Baldo-Ceolin (Ed.), Proc. 8-th Int. Workshop on Neutrino Telescopes, Papergraf pub., vol. II, 1999, p. 239.
[19] R.H. Helm, Phys. Rev. 104 (1956) 1466; A. Bottino et al., Astrop. Phys. 2 (1994) 77.
[20] M. Ambrosio et al., Astrop. Phys. 7 (1997) 109.
[21] Particle Data Group: Review of Particle Physics, Eur. Phys. J. C 3 (1998) 1.
[22] P.J.T. Leonard, S. Tremaine, Astrophys. J 353 (1990) 486; C.S. Kochanek, Astrophys. J 457 (1996) 228; K.M. Cudworth, Astron. J 99 (1990) 590.
[23] K. Hikasa et al., Phys. Rev. D 45 (1992) III 38.
[24] G.J. Feldman, R.D. Cousins, Phys. Rev. D 57 (1998) 3873.